CAPILLARY CONVECTION IN A LIQUID LAYER ON EXPOSURE TO LASER RADIATION

V. V. Nizovtsev

UDC 532.62

The dimensions of a convection cell, the profile of the depression on the layer surface, the velocity of the steady-state liquid motion, and the dynamics of the development of the convection in liquid layers with different viscosity are determined.

High sensitivity of liquids to shearing tensions was used in solving such technical problems as separation of impurities [1], obtaining relief photographic images [2, 3], deposition of a substance in a prescribed zone of a substrate [4], or the surface alloying of metals [5]. The enumerated technical solutions are based on capillary convection controlled by the thermal action of the radiation [6, 7]. In spite of the wide sphere of possible applications of forced capillary convection, the quantitative data on this problem are practically absent in the literature due to experimental difficulties. Below, the results of research on capillary convection under the local influence of low-power laser radiation are presented.

In this work, dye solutions of crystal violet were used in polar organic solutions (Table 1). The dye contrasted with the image of the relief on the surface of the layer and served as an agent absorbing the radiation. Thermocapillary convection was induced by the action of a Gaussian beam of radiation produced by a helium–neon laser with 1 mW in power, where the beam diameter in the plane of the layer was about 1 mm. A dye concentration of 10 g/liter has been chosen so as to provide an optical density equal to 1 in the region of 633 nm in a layer of thickness less than 0.1 mm. Liquids were applied on substrates from polymethylmethacrylate, silicate glass, and brass with thermal conductivities 0.2, 1.0, and 100 W/(m·K), respectively. The velocity of motion of liquid particles at the surface and the convective cell diameter were determined with the help of motion-picture and still photography in the reflected light of the lycopodium suspension layer in the examined solution. The relief on the liquid surface was determined by means of microphotometering the photographic images of the layer obtained in the transmitted light.

Parameters of Convection Cell. Convection, which is thermal and concentrational in nature, can be expected to arise under the action of the radiation because the coefficient of the surface tension depends both on temperature and concentration of the solution. The difference in σ between surface zones with different temperatures and concentrations is equal to

$$\delta\sigma = \sigma_T'\delta T + \sigma_C'\delta C = \delta\sigma_T + \delta\sigma_C . \qquad (1)$$

For the solutions used $\sigma'_T \approx -0.1$ mN/(m·K); $\sigma'_C \approx 0.1$ N·liter/(m·kg) [12].

Local heating of the surface layer of liquid causes convection due to the thermocapillary effect. A decrease in the surface tension in the irradiated zone leads to the formation of centrifugal surface flows, which, due to the finite viscosity of the liquid, form the relief in the shape of a depression surrounded by a ridge. The difference in the capillary Laplace pressures that arises between the toroidal zone of the ridge and the center of the irradiated zone of the surface determines the backward flows in the lower part of the layer. For the layer thicknesses examined, the gravitational convection can be neglected because the Bond number, determined as the ratio of hydrostatic forces to capillary forces, does not exceed 0.1. The same conclusion about the prevailing role of capillary forces in the laser processing of metal surfaces is presented in [13].

In Fig. 1a, an axial cross section of the depression is shown for a layer of solution in butanol. The location of the nonperturbed surface is marked conventionally because the

---

M. V. Lomonosov Moscow State University. Translated from Inzhenerno-Fizicheskii Zhurnal Vol. 55, No. 1, pp. 85-92, July, 1988. Original article submitted February 27, 1987.

0022-0841/88/5501-0767$12.50

TABLE 1. Properties of Solvents and Parameters of Thermocapillary Convection

Solvent	Viscosity, 10^{-3} Pa·sec, °C [8, 9]	Surface tension at 20°C, mN/m [10, 11]	Termal coefficient of surface tension, mN/m·K [11]	Boiling point, °C	Velocity of liquid motion on the surface, mm/sec	The constant of cell formation velocity, sec^{-1}
Acetone	0,32 20	23,7	—0,112	56,2		
1,2-dichlorethane	0,80 25	32,5	—0,143	83,5		
Ethanol	1,08 25	22,8	—0,083	78,3	4,8±1,6	3,1
Butanol	2,95 20	24,6	—0,090	117,9	2,0±0,5	1,7; 2,5; 3,6
Octanol	7,6 25	27,5	—0,079	194,5	0,5±0,2	1,8
Ethylene glycol	18,5 22	48,5	—0,089	197,0		
Cyclohexanol	68,0 20	26,5	—0,097		0,25±0,05	2,0

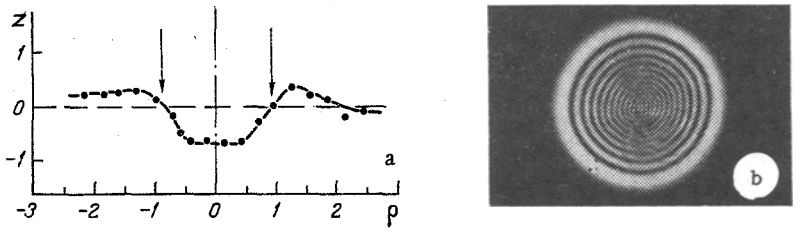

Fig. 1. Profile of the depression on a 0.3-mm-thick layer on glass (a), and a perpendicular cross section of the beam of radiation reflected by the layer (b). The arrows show the beam boundaries determined from the intensity equal to 0.1 of maximum. z, μm; ρ, mm.

profile has an asymmetric form due to surface convection related to vaporization [14]. The size of the convective space depends weakly on the liquid viscosity and is determined by the layer thickness and the light beam diameter. It is important to note that the cell diameter depends weakly on the thermal conduction of the substrate and on the radiation power. The results obtained for liquids of different viscosity demonstrate that the dependence of the cell radius on the layer thickness in the range of 0.1-0.5 mm can be described by the approximate formula $r \approx r_b + 1.5\ h$.

Relief at the Bottom of the Depression. The power distribution obtained in the cross section of the reflected beam is clearly interferential in nature (Fig. 1). Theoretically and in the most general form this question was earlier considered in [15]; however, the experimental aspect was examined only qualitatively. It was suggested in [15, 16] that the obtained pattern of the radiation distribution was the result of interference of the beams reflected by the depression itself and by a convex toroidal mirror of the ridge around it. However, the ratio of the beam width and the size of the deformed surface area (Fig. 1) indicates that the ridge, surrounding the depression, does not show itself in the interference picture since it is positioned beyond the boundaries of the radiant beam.

In Fig. 2, the dynamics of variation of the power distribution is shown in the cross section of the reflected beam. Curves 1 and 2 indicate that during approximately 1/20 sec of irradiation, there is no noticeable deformation of the liquid surface; however, one can observe an increase in the reflected power by several times. The increase in the reflection coefficient during the first moments of radiation is explained by the increase in the coefficient of absorption of surface liquid layers due to the local vaporization of the solution and increase in the concentration of the dye on the surface [17]. At subsequent stages of radiation this local gradient in the solution concentration vanishes due to convective intermixing of the liquid. Further radiation results in disintegration of the Gaussian power distribution in the reflected beam into a number of concentric bands.

Microphotometric measurements on the images of the deformed surface zone, obtained after their contrast enhancement, have detected a weakly defined convexity in the center of the depression. In Fig. 3, a microphotogram of a double-positive image of the cell is shown, the profile of which is given in Fig. 1. The relief on the surface of the layer is in the form of a cup. With allowance for the nature of the liquid motion in the cell, the detected

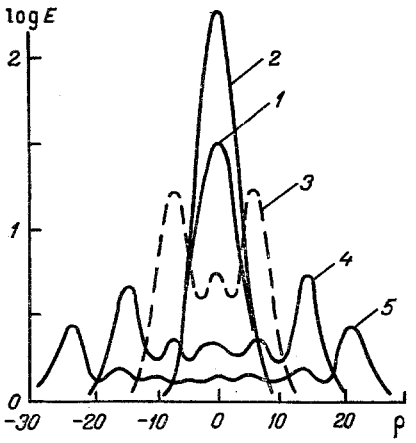

Fig. 2

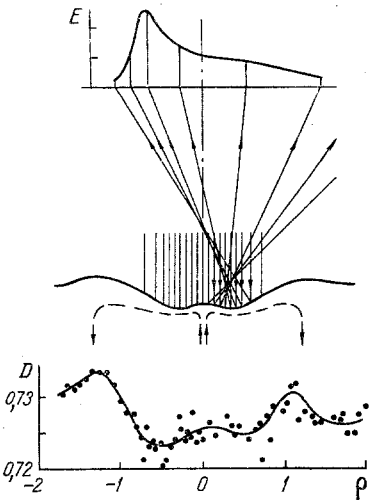

Fig. 3

Fig. 2. Microphotographs of the interference pattern in the cross section of the beam reflected by a layer of solution in cyclohexanol, 3 mm in thickness. The frequency of the motion-picture filming is 16 frames/sec; the numbers by the curves are the frame numbers; the distance from the layer is 3 m.

Fig. 3. Profile reconstructed from the microphotogram and the expected illumination distribution E in the cross section of the beam reflected by one side of the profile.

singularity of the profile should not be surprising. Indeed, in the center of the deformed zone of the surface, the liquid particles abruptly change their direction of motion from vertically upward to horizontal (dashed lines in Fig. 3). In the process, the hydrodynamic pressure of the arrested jet is balanced by the Laplace pressure of a convex meniscus. The power distribution in the cross section of the beam in Fig. 1b is the result of interference of the bell-shaped distributions, one of which is shown in Fig. 3.

The divergence of the reflected beams and, consequently, the diameter of the interference pattern, are determined by the curvature of the toroidal trough at the bottom of the depression, which, in turn, depends on the overall cell dimensions and on the sharpness of the central meniscus at the center of the depression. It was noticed above that when the thickness of the layer decreases, the convection cell diameter contracts and, therefore, the side walls of the depression are brought closer together, thus increasing the curvature of the toroidal mirror at the bottom. In fact, it follows from Fig. 4 that the cross-sectional diameter of the reflected beam changes in inverse proportion to the layer thickness. The relief sharpens also when the power of the incident radiation increases. Independent of the substrate material and properties of the liquid, the cross-sectional diameter depends linearly on the power. All other things being equal, the sharpness of the meniscus and the image diameter depend on the velocity of liquid motion, which, in turn, is determined by the radiation power and viscosity.

As is seen from Fig. 1, when the density of the delivered power is approximately 1 mW/mm^2, the gradient of the layer thickness is about 1 μm/mm. When this value is compared with the results of [18], in which the convection was caused by nonuniform heating of the substance, our attention is drawn to the significant difference between the depths of the relief resulting from the thermocapillary convection. In [18], the gradient of the layer thickness is higher by an order of magnitude. The cause for the deviation can be found by comparing indirectly the powers delivered to the layer in the two given cases. It was noticed in [18] that when the layer thickness was small the process resulted in exposure of the metal substrate. In our experiments, with the same thicknesses, this was observed only for the polymethyacrylate substrate. By comparing the thermal conductivities of the substrate materials, one can conclude that in the cited work the density of the power delivered to the layer was at least an order of magnitude higher; therefore, the difference in the sharpness of the relief is valid.

Mass Transfer in Convection. Table 1 lists the experimental values of the velocities v_i of liquid motion on the surface of the cell at the inflection point on the side wall of the depression with the 0.35-mm-thick layer on the glass. A decrease in the radiant power by a factor of five is followed by a nearly fivefold decrease in velocity. In the case of butanol, when the thickness is equal to 0.15 mm, the velocity is equal to 0.9 ± 0.2 mm/sec. An increase in viscosity and decrease in the layer thickness have a negative effect on the convection velocity. These results correspond to [19] and contradict the conclusions drawn in [20].

In order to estimate the velocity on the layer surface we assume that in the cross section of the convective cycle under the inflection point at a distance from the beam axis approximately equal to r/2, the velocity is distributed linearly along the vertical direction in a centrifugal flow and the velocity is distributed parabolically in a backward flow [21, 18]. The backward flow results from the difference of pressures $p_2 - p_1$ in the peripheral and contral zones of the cell. The velocities on the substrate and at a certain height 2a above the substrate are equal to zero. We place the origin of the vertical z axis at a height a above the substrate. Then

$$v_1 = B(z-a); \qquad a \leqslant z \leqslant h-a; \tag{2}$$

$$v_2 = -\frac{a^2}{2b\mu}(p_2 - p_1)[1-(z/a)^2]; \quad |z| \leqslant a. \tag{3}$$

The backward flow above the inflection point can be assumed to depend on the average gradient of the Laplace pressure

$$(p_2 - p_1)/b \approx \sigma(1/R_2 + 2/R_1)/r. \tag{4}$$

From the condition of matching the derivatives of functions (2) and (3) at the point a, it follows that

$$B = \frac{a\sigma}{\mu r}\left(\frac{1}{R_2} + \frac{2}{R_1}\right).$$

Starting from the equality of the three-dimensional flow rates in the centrifugal and backward directions, we obtain similarly to [22] that a = h/3. The velocity v_i is determined from the expression

$$v_i = \frac{h^2\sigma}{9\mu r}\left(\frac{2}{R_1} + \frac{1}{R_2}\right). \tag{5}$$

The radii were determined from graphs analogous to those in Fig. 1. Due to the reasons mentioned above, the relative error of these calculations was about 30%. For butanol with a thickness 0.25 and 0.35 mm the average values of the radii of curvature are equal and are about 0.5 m. For these thicknesses, (5) gives values of velocities of 0.25 and 0.5 mm/sec respectively. The calculated values are close to the experimental ones, which are equal to 0.3 ± 0.1 and 2.0 ± 0.5 mm/sec.

The flow is laminar on every segment of the convection path. Even for liquids with low viscosity, for which the velocity on the surface is of the order of 10 mm/sec, Re does not exceed 5 for the centrifugal flow and 25 for the vertical pipe in the center of the cell.

Kinetics of the Formation of the Convection Cell. The time for the formation of the cell with the stationary profiles of the surface and velocity depends on properties of both the liquid and substrate. The kinetics of the development of convection has been investigated by analyzing variations in the geometry of the beam reflected by the depression. The behavior of the interference pattern diameter (see Fig. 2) is governed by the variation in curvature of the layer surface; consequently, it reflects the dynamics of formation of the cell. In Table 1, the values of the velocity constant are given for the cell formation in a layer 0.3 mm in thickness on the glass. For the case of butanol, the constants are given for the layer on the polymethylmethacrylate, glass, and brass, respectively. The pattern diameter in processing data was assumed to vary with time according to the law

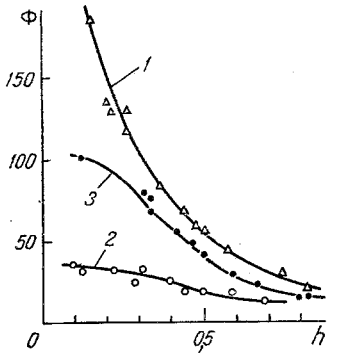

Fig. 4. Dependence of the diameter Φ (mm) of the interference pattern on the thickness h (mm) of the layer of ethanol (1), ethylene glycol (2), and cyclohexanol (3) on the glass. The diameter is measured at a distance of 6 m from the layer.

$$\Phi = \Phi_s [1 - \exp(-kt)]. \quad (6)$$

The kinetics is well described by Eq. (6) up to the values $\Phi \approx 0.8\ \Phi_s$; after these values have been attained, the process slows down somewhat.

The constant is proportional to the beam power and the thermal conductivity of the substrate. The latter confirms that in attaining a stationary state the convective heat transfer from the upper liquid layer heated by the radiation to the substrate plays an important role. The cell formation is completed when a constant temperature gradient between the surface zones in the center of the cell and on its periphery is attained. The higher the thermal conductivity, the lower is the gradient and the faster it is attained. When the coefficient of the thermal conductivity on the substrate material is equal to the thermal conductivity of the liquid, the cell formation is decelerated and in general becomes impossible for a volatile solvent (acetone, dichloroethane). When the layer thickness is less than 0.3 mm and the power is equal to 1 mW, the layer is disrupted after 20 sec of exposure to radiation due to the accumulation of heat, gain in convection, and vaporization of the solvent. The convection changes in nature, transforming from thermocapillary convection into concentrational convection, because the absolute value of the second term in (1) becomes larger than the first term. In the center of the irradiated zone of the exposed substrate, a drop of the concentrate is collected, which absorbs the radiant energy and creates an axially symmetrical temperature gradient around itself in the substrate. The latter sustains a centripetal flow of the liquid to the drop in the shape of jets and small drops. For the limited volume of the gaseous phase and long-term irradiation, the dissolved substance accumulates in the center of the irradiated zone, while the pure solvent is left in the cold zones of the substrate. A concentrational convection is considered in [1, 23].

Use of Capillary Convection Controllable by the Thermal Action of Light. The results obtained allow us to understand the essence of the effects that underlie new technical solutions [2, 4] and to estimate the values of the parameters that characterize these solutions.

Starting from data on the kinetics and the radiant power, we can obtain the value of the exposure required for the forming of the image in the shape of the relief on the liquid layer. An estimate shows that even for the liquids from the upper part of Table 1 the exposure is of the order of 10 mJ/cm^2. The experiments based on the recording of hatched images support this conclusion. Under such an exposure and somewhat longer exposure, a positive relief self-erasing image is formed, with resolving power not exceeding 20 mm^{-1}. The low resolving power results from the fact that the neighbor cells mutually suppress each other during the thermocapillary convection. When the exposure is continued until complete evaporation of the solvent, a transition to concentrational convection is observed, and a negative fixed image is formed. The exposure required for this is about 1 J/cm^2, and the resolving power reaches 500 mm^{-1} [6].

It is known that as a whole the depth of the relief of convective nature on the surface layer of the liquid does not depend on viscosity [24]. The results of investigations, however, demonstrate that contactless determination of the viscosity is possible by means of the measurement of the interference pattern diameter in the reflected beam [25]. The presence of a meniscus in the center of the depression, the sharpness of which depends on the velocity of the convection and, consequently, on the viscosity, allows us to determine the viscosity from the cross-sectional diameter of the reflected beam. Unfortunately, determining the viscosity by this method is possible only when the surface tension is known, because the shape of the meniscus at the bottom of the depression depends also on the surface tension. In Fig. 4, curve 2 represents the dependence of the cross-sectional diameter on the layer thickness for ethylene glycol. As is seen, the diameter for all the thicknesses is considerably less than for the case of cyclohexanol, the viscosity of which is higher, which results from the raised surface tension of the ethylene glycol.

NOTATION

a, coordinate of point on the z axis at which the liquid velocity is equal to 0; B, constant in Eq. (2); b, large radius of the toroid, equal approximately to r; C, concentration of the solution; D, optical density; E, illumination in the cross section of the beam reflected by the layer; h, thickness of the layer; k, velocity constant of variation of diameter Φ; ℓ, convective path length in the centrifugal direction beyond the radiant beam; p_1 and p_2, pressures at the cell center and under the ridge of the toroid around the depression; R_1 and R_2, radii of curvature of the layer surface at the center and of the ridge on the cell periphery; Re, Reynolds number; r, convective cell radius; r_b, radiant beam radius; t, time; T, temperature; v_1 and v_2, calculated centrifugal and backward velocities of the liquid in the cell cross section corresponding to the inflection point on the layer surface; v_i, liquid velocity at the inflection point; W, radiant power, z, vertical axis originating at a point at a height a from the substrate surface; σ, surface-tension coefficient; σ'_C and σ'_T, mean coefficients of the concentration and temperature dependences of σ; δ, increments in the quantities in the irradiated zone; μ, dynamic viscosity of the liquid; Φ, diameter of the interference pattern in the cross section of the reflected beam; Φ_s, steady-state value of Φ.

LITERATURE CITED

1. B. A. Bezuglyi, E. A. Galashin, D. P. Krindach, and V. S. Maiorov, Pis'ma Zh. Tekh. Fiz., 2, No. 18, 832-838 (1976).
2. B. A. Bezuglyi and E. A. Galashin, Zh. Nauch. Prikl. Fotogr. Kinematogr., 27, No. 1, 69-72 (1982).
3. "Reprographic photosensitive material," Inventor's Cert. No. 1113774 SSSR, MKI^3 G 03 C 1/72.
4. A. B. Bezuglyi, E. A. Galashin, and A. N. Fedotov, Zh. Nauch. Prikl. Fotogr. Kinematogr., 22, No. 1, 3-9 (1977).
5. I. B. Borovskii, D. D. Gorodskii, I. M. Sharafeev, and S. F. Moryashchev, Fiz.-Khim. Obrab. Mater., No. 1, 19-23 (1984).
6. B. A. Bezyglyi, "Capillary convection controlled by the thermal action of light and its application in the means of information registration," Author's Abstract of Candidate's Dissertation, Phys.-Mat. Sci., Moscow (1985).
7. A. T. Sukhodol'skii, Izv. Akad. Nauk SSSR, Ser. Fiz., 50, No. 6, 1095-1102 (1986).
8. B. P. Nikol'skii (ed.), Chemist's Handbook [in Russian], Vol. 1, Moscow–Leningrad (1977).
9. A. Gordon and R. Ford, Chemist's Guide [in Russian], Moscow (1976).
10. N. B. Vargaftik, A Handbook on Thermophysical Properties of Gases and Liquids [in Russian], Moscow (1972).
11. A. A. Abramzon and E. D. Shchukina (eds.), Surface Phenomena and Surface-Active Substances (Handbook) [in Russian], Leningrad (1984).
12. V. V. Nizovtsev and N. P. Netesova, Colloid. J., 47, No. 5, 975-978 (1985).
13. H. E. Cline, J. Appl. Phys., 52, No. 1, 443-448 (1981).
14. V. V. Nizovtsev and N. P. Netesova, Colloid. J., 47, No. 6, 1196-1200 (1985).
15. Da Costa G., Calatroni J., Appl. Opt., 18, No. 2, 233-240 (1979).
16. Da Costa G., Physics Lett., 80a, No. 4, 323-324 (1980).
17. R. W. Ditchburn, Light [Russian translation], Moscow (1965).
18. A. F. Pshenichnikov and G. A. Tokmenina, Izv. Akad. Nauk SSSR, Mekh. Zhidk Gaza, No. 3, 150153 (1983).

19. R. V. Birikh, Zh. Prikl. Mekh. Tekh. Fiz., No. 3, 69-72 (1966).
20. Yu. V. Sanochkin, Zh. Prikl. Mekh. Tekh. Fiz., No. 6, 134-137 (1983).
21. R. Bird, W. E. Stewart, and E. N. Lightfoot, Transport Phenomena, Wiley (1960).
22. Yu. V. Sanochkin, Isv. Akad. Nauk SSSR, Mekh. Zhidk. Gaza, No. 6, 146-152 (1984).
23. B. A. Bezuglyi and V. V. Nizovtsev, Vestn. Mosk. Univ., Ser. Fiz. Astron., 22, No. 6, 37-41 (1981).
24. L. D. Landau and E. M. Lifshits, Mechanics of Continuous Media [in Russian], 2nd ed., Moscow (1954).
25. "A method for determining viscosity," Inventor's Certificate No. 1188588 SSSR: MKI^3 G 01 N 11/16.